
Bayesian Deep Ensembles via the Neural Tangent Kernel

Bobby He

Department of Statistics
University of Oxford
bobby.he@stats.ox.ac.uk

Balaji Lakshminarayanan

Google Research
Brain team
balajiln@google.com

Yee Whye Teh

Department of Statistics
University of Oxford
y.w.teh@stats.ox.ac.uk

Abstract

We explore the link between deep ensembles and Gaussian processes (GPs) through the lens of the Neural Tangent Kernel (NTK): a recent development in understanding the training dynamics of wide neural networks (NNs). Previous work has shown that even in the infinite width limit, when NNs become GPs, there is no GP posterior interpretation to a deep ensemble trained with squared error loss. We introduce a simple modification to standard deep ensembles training, through addition of a computationally-tractable, randomised and untrainable function to each ensemble member, that enables a posterior interpretation in the infinite width limit. When ensembled together, our trained NNs give an approximation to a posterior predictive distribution, and we prove that our Bayesian deep ensembles make more conservative predictions than standard deep ensembles in the infinite width limit. Finally, using finite width NNs we demonstrate that our Bayesian deep ensembles faithfully emulate the analytic posterior predictive when available, and can outperform standard deep ensembles in various out-of-distribution settings, for both regression and classification tasks.

1 Introduction

Consider a training dataset \mathcal{D} consisting of N i.i.d. data points $\mathcal{D} = \{\mathcal{X}, \mathcal{Y}\} = \{(\mathbf{x}_n, y_n)\}_{n=1}^N$, with $\mathbf{x} \in \mathbb{R}^d$ representing d -dimensional features and y representing C -dimensional targets. Given input features \mathbf{x} and parameters $\boldsymbol{\theta} \in \mathbb{R}^p$ we use the output, $f(\mathbf{x}, \boldsymbol{\theta}) \in \mathbb{R}^C$, of a neural network (NN) to model the predictive distribution $p(y|\mathbf{x}, \boldsymbol{\theta})$ over the targets. For univariate regression tasks, $p(y|\mathbf{x}, \boldsymbol{\theta})$ will be Gaussian: $-\log p(y|\mathbf{x}, \boldsymbol{\theta})$ is the squared error $\frac{1}{2\sigma^2}(y - f(\mathbf{x}, \boldsymbol{\theta}))^2$ up to additive constant, for fixed observation noise $\sigma^2 \in \mathbb{R}_+$. For classification tasks, $p(y|\mathbf{x}, \boldsymbol{\theta})$ will be a Categorical distribution.

Given a prior distribution $p(\boldsymbol{\theta})$ over the parameters, we can define the posterior over $\boldsymbol{\theta}$, $p(\boldsymbol{\theta}|\mathcal{D})$, using Bayes' rule and subsequently the *posterior predictive* distribution at a test point (\mathbf{x}^*, y^*) :

$$p(y^*|\mathbf{x}^*, \mathcal{D}) = \int p(y^*|\mathbf{x}^*, \boldsymbol{\theta})p(\boldsymbol{\theta}|\mathcal{D}) d\boldsymbol{\theta} \quad (1)$$

The posterior predictive is appealing as it represents a marginalisation over $\boldsymbol{\theta}$ weighted by posterior probabilities, and has been shown to be optimal for minimising predictive risk under a well-specified model [1]. However, one issue with the posterior predictive for NNs is that it is computationally intensive to calculate the posterior $p(\boldsymbol{\theta}|\mathcal{D})$ exactly. Several approximations to $p(\boldsymbol{\theta}|\mathcal{D})$ have been introduced for *Bayesian neural networks* (BNNs) including: Laplace approximation [2]; Markov chain Monte Carlo [3, 4]; variational inference [5–9]; and Monte-Carlo dropout [10].

Despite the recent interest in BNNs, it has been shown empirically that deep ensembles [11], which lack a principled Bayesian justification, outperform existing BNNs in terms of uncertainty quantification and out-of-distribution robustness, cf. [12]. Deep ensembles independently initialise

Preprint. Under review.

and train individual NNs (referred to herein as *baselearners*) on the negative log-likelihood loss $\mathcal{L}(\boldsymbol{\theta}) = \sum_{n=1}^N \ell(y_n, f(\mathbf{x}_n, \boldsymbol{\theta}))$ with $\ell(y, f(\mathbf{x}, \boldsymbol{\theta})) = -\log p(y|\mathbf{x}, \boldsymbol{\theta})$, before aggregating predictions. Fort et al. [13] suggested that the success of deep ensembles is explained by their ability to explore different functional modes, while Wilson and Izmailov [14] argued that deep ensembles are actually approximating the posterior predictive.

Our contribution will be to combine deep ensembles with recent developments connecting GPs and wide NNs, both before [15–19] and after [20, 21] training. Using these insights, we devise a modification to standard NN training that yields an exact posterior sample for $f(\cdot, \boldsymbol{\theta})$ in the infinite width limit. As a result, when ensembled together our modified baselearners give a posterior predictive approximation, and can thus be viewed as a *Bayesian deep ensemble*.

One concept that is related to our methods concerns ensembles trained with *Randomised Priors* to give an approximate posterior interpretation, which we will use when modelling observation noise in regression tasks. The idea behind randomised priors is that, under certain conditions, regularising baselearner NNs towards independently drawn “priors” during training produces exact posterior samples for $f(\cdot, \boldsymbol{\theta})$. Randomised priors recently appeared in machine learning applied to reinforcement learning [22] and uncertainty quantification [23], like this work. To the best of our knowledge, related ideas first appeared in astrophysics where they were applied to Gaussian random fields [24]. However, one such condition for posterior exactness with randomised priors is that the model $f(\mathbf{x}, \boldsymbol{\theta})$ is linear in $\boldsymbol{\theta}$. This is not true in general for NNs, but has been shown to hold for wide NNs local to their parameter initialisation, in a recent line of work. In order to introduce our methods, we will first review this line of work, known as the *Neural Tangent Kernel* (NTK) [20].

2 NTK Background

Wide NNs, and their relation to GPs, have been a fruitful area recently for the theoretical study of NNs: we review only the most salient developments to this work, due to limited space.

First introduced by Jacot et al. [20], the *empirical NTK* of $f(\cdot, \boldsymbol{\theta}_t)$ is, for inputs \mathbf{x}, \mathbf{x}' , the kernel:

$$\hat{\Theta}_t(\mathbf{x}, \mathbf{x}') = \langle \nabla_{\boldsymbol{\theta}} f(\mathbf{x}, \boldsymbol{\theta}_t), \nabla_{\boldsymbol{\theta}} f(\mathbf{x}', \boldsymbol{\theta}_t) \rangle \quad (2)$$

and describes the functional gradient of a NN in terms of the current loss incurred on the training set. Note that $\boldsymbol{\theta}_t$ depends on a random initialisation $\boldsymbol{\theta}_0$, thus the empirical NTK is random for all $t > 0$.

Jacot et al. [20] showed that for an MLP under a so-called NTK parameterisation, the empirical NTK converges in probability to a deterministic limit, Θ , that stays constant during gradient training, as the hidden layer widths of the NN go to infinity sequentially. Later, Yang [25] extended the NTK convergence results to convergence almost surely, which is proven rigorously for a variety of architectures and for widths (or channels in Convolutional NNs) of hidden layers going to infinity in unison. This limiting positive-definite (p.d.) kernel Θ , known as the NTK, depends only on certain NN architecture choices, including: activation, depth and variances for weight and bias parameters. Note that the NTK parameterisation, detailed in Appendix A, can be thought of as akin to training under standard parameterisation with a learning rate that is inversely proportional to the width of the NN, which has been shown to be the largest scale for stable learning rates in wide NNs [26–28].

Lee et al. [21] built on the results of Jacot et al. [20], and studied the *linearised regime* of an NN. Specifically, if we denote as $f_t(\mathbf{x}) = f(\mathbf{x}, \boldsymbol{\theta}_t)$ the network function at time t , we can define the first order Taylor expansion of the network function around randomly initialised parameters $\boldsymbol{\theta}_0$ to be:

$$f_t^{\text{lin}}(\mathbf{x}) = f_0(\mathbf{x}) + \nabla_{\boldsymbol{\theta}} f(\mathbf{x}, \boldsymbol{\theta}_0) \Delta \boldsymbol{\theta}_t \quad (3)$$

where $\Delta \boldsymbol{\theta}_t = \boldsymbol{\theta}_t - \boldsymbol{\theta}_0$ and $f_0 = f(\cdot, \boldsymbol{\theta}_0)$ is the randomly initialised NN function.

For notational clarity, whenever we evaluate a function at an arbitrary input set \mathcal{X}' instead of a single point \mathbf{x}' , we suppose the function is vectorised. For example, $f_t(\mathcal{X}) \in \mathbb{R}^{NC}$ denotes the concatenated NN outputs on training set \mathcal{X} , whereas $\nabla_{\boldsymbol{\theta}} f_t(\mathcal{X}) = \nabla_{\boldsymbol{\theta}} f(\mathcal{X}, \boldsymbol{\theta}_t) \in \mathbb{R}^{NC \times p}$. In the interest of space, we will also sometimes use subscripts to signify kernel inputs, so for instance $\Theta_{\mathbf{x}', \mathcal{X}} = \Theta(\mathbf{x}', \mathcal{X}) \in \mathbb{R}^{C \times NC}$ and $\Theta_{\mathcal{X}, \mathcal{X}} = \Theta(\mathcal{X}, \mathcal{X}) \in \mathbb{R}^{NC \times NC}$ throughout this work.

The results of Lee et al. [21] showed that in the infinite width limit, with NTK parameterisation and gradient flow under squared error loss, $f_t^{\text{lin}}(\mathbf{x})$ and $f_t(\mathbf{x})$ are equal for any $t \geq 0$, for a shared random

initialisation θ_0 . In particular, for the linearised network it can be shown, that as $t \rightarrow \infty$:

$$f_\infty^{\text{lin}}(\mathbf{x}) = f_0(\mathbf{x}) - \hat{\Theta}_0(\mathbf{x}, \mathcal{X}) \hat{\Theta}_0(\mathcal{X}, \mathcal{X})^{-1} (f_0(\mathcal{X}) - \mathcal{Y}) \quad (4)$$

and thus as the hidden layer widths converge to infinity we have that:

$$f_\infty^{\text{lin}}(\mathbf{x}) = f_\infty(\mathbf{x}) = f_0(\mathbf{x}) - \Theta(\mathbf{x}, \mathcal{X}) \Theta(\mathcal{X}, \mathcal{X})^{-1} (f_0(\mathcal{X}) - \mathcal{Y}) \quad (5)$$

We can replace $\Theta(\mathcal{X}, \mathcal{X})^{-1}$ with the generalised inverse when invertibility is an issue. However, this will not be a main concern of this work, as we will mostly add regularisation that corresponds to modelling observation/output noise, which ensures invertibility.

From Eq. (5) we see that, conditional on the training data $\{\mathcal{X}, \mathcal{Y}\}$, we can decompose f_∞ into $f_\infty(\mathbf{x}) = \mu(\mathbf{x}) + \gamma(\mathbf{x})$ where $\mu(\mathbf{x}) = \Theta(\mathbf{x}, \mathcal{X}) \Theta(\mathcal{X}, \mathcal{X})^{-1} \mathcal{Y}$ is a deterministic mean and $\gamma(\mathbf{x}) = f_0(\mathbf{x}) - \Theta(\mathbf{x}, \mathcal{X}) \Theta(\mathcal{X}, \mathcal{X})^{-1} f_0(\mathcal{X})$ captures predictive uncertainty, due to the randomness of f_0 . Now, if we suppose that, at initialisation, $f_0 \stackrel{d}{\sim} \mathcal{GP}(0, k)$ for an arbitrary kernel $k : \mathbb{R}^d \times \mathbb{R}^d \rightarrow \mathbb{R}^{C \times C}$, then we have $f_\infty(\cdot) \stackrel{d}{\sim} \mathcal{GP}(\mu(\mathbf{x}), \Sigma(\mathbf{x}, \mathbf{x}'))$ for two inputs \mathbf{x}, \mathbf{x}' , where:¹

$$\Sigma(\mathbf{x}, \mathbf{x}') = k_{\mathbf{x}\mathbf{x}'} + \Theta_{\mathbf{x}\mathcal{X}} \Theta_{\mathcal{X}\mathcal{X}}^{-1} k_{\mathcal{X}\mathcal{X}} \Theta_{\mathcal{X}\mathcal{X}}^{-1} \Theta_{\mathcal{X}\mathbf{x}} - (\Theta_{\mathbf{x}\mathcal{X}} \Theta_{\mathcal{X}\mathcal{X}}^{-1} k_{\mathcal{X}\mathbf{x}'} + h.c.) \quad (6)$$

For a generic kernel k , Lee et al. [21] observed that this limiting distribution for f_∞ does not have a posterior GP interpretation unless k and Θ are multiples of each other, .

As mentioned in Section 1, previous work [15–19] has shown that there is a distinct but closely related kernel \mathcal{K} , known as the *Neural Network Gaussian Process* (NNGP) kernel, such that $f_0 \stackrel{d}{\sim} \mathcal{GP}(0, \mathcal{K})$ at initialisation in the infinite width limit and $\mathcal{K} \neq \Theta$. Thus Eq. (6) with $k=\mathcal{K}$ tells us that, for wide NNs under squared error loss, there is no Bayesian posterior interpretation to a trained NN, nor is there an interpretation to a trained deep ensemble as a Bayesian posterior predictive approximation.

3 Proposed modification to obtain posterior samples in infinite width limit

Lee et al. [21] noted that one way to obtain a posterior interpretation to f_∞ is by randomly initialising f_0 but only training the parameters in the final linear readout layer, as the contribution to the NTK Θ from the parameters in final hidden layer is exactly the NNGP kernel \mathcal{K} .² f_∞ is then a sample from the GP posterior with prior kernel NNGP, \mathcal{K} , and noiseless observations in the infinite width limit i.e. $f_\infty(\mathcal{X}') \stackrel{d}{\sim} \mathcal{N}(\mathcal{K}_{\mathcal{X}'\mathcal{X}} \mathcal{K}_{\mathcal{X}\mathcal{X}}^{-1} \mathcal{Y}, \mathcal{K}_{\mathcal{X}'\mathcal{X}'} - \mathcal{K}_{\mathcal{X}'\mathcal{X}} \mathcal{K}_{\mathcal{X}\mathcal{X}}^{-1} \mathcal{K}_{\mathcal{X}\mathcal{X}'})$. This is an example of the ‘‘sample-then-optimize’’ procedure of Matthews et al. [29], but, by only training the final layer this procedure limits the earlier layers of an NN solely to be random feature extractors.

We now introduce our modification to standard training that trains all layers of a finite width NN and obtains an exact posterior interpretation in the infinite width limit with NTK parameterisation and squared error loss. For notational purposes, let us suppose $\theta = \text{concat}(\{\theta^{\leq L}, \theta^{L+1}\})$ with $\theta^{\leq L} \in \mathbb{R}^{p-p_{L+1}}$ denoting L hidden layers, and $\theta^{L+1} \in \mathbb{R}^{p_{L+1}}$ denoting final readout layer $L+1$. Moreover, define $\Theta^{\leq L} = \Theta - \mathcal{K}$ to be the p.d. kernel corresponding to contributions to the NTK from all parameters before the final layer, and $\hat{\Theta}_t^{\leq L}$ to be the empirical counterpart depending on θ_t . To motivate our modification, we reinterpret f_t^{lin} in Eq. (3) by splitting terms related to \mathcal{K} and $\Theta^{\leq L}$:

$$f_t^{\text{lin}}(\mathbf{x}) = \underbrace{f_0(\mathbf{x}) + \nabla_{\theta^{L+1}} f(\mathbf{x}, \theta_0) \Delta \theta_t^{L+1}}_{\mathcal{K}} + \underbrace{\mathbf{0}_C + \nabla_{\theta^{\leq L}} f(\mathbf{x}, \theta_0) \Delta \theta_t^{\leq L}}_{\Theta - \mathcal{K}} \quad (7)$$

where $\mathbf{0}_C \in \mathbb{R}^C$ is the zero vector. As seen in Eq. (7), the distribution of $f_0^{\text{lin}}(\mathbf{x}) = f_0(\mathbf{x})$ lacks extra variance, $\Theta^{\leq L}(\mathbf{x}, \mathbf{x})$, that accounts for contributions to the NTK Θ from all parameters $\theta^{\leq L}$ before the final layer. This is precisely why no Bayesian interpretation exists for a standard trained wide NN, as in Eq. (6) with $k=\mathcal{K}$. The motivation behind our modification is now very simple: we propose to manually add in this missing variance. Our modified NNs, $\tilde{f}(\cdot, \theta)$, will then have trained distribution:

$$\tilde{f}_\infty(\mathcal{X}') \stackrel{d}{\sim} \mathcal{N}(\Theta_{\mathcal{X}'\mathcal{X}} \Theta_{\mathcal{X}\mathcal{X}}^{-1} \mathcal{Y}, \Theta_{\mathcal{X}'\mathcal{X}'} - \Theta_{\mathcal{X}'\mathcal{X}} \Theta_{\mathcal{X}\mathcal{X}}^{-1} \Theta_{\mathcal{X}\mathcal{X}'}) \quad (8)$$

¹Throughout this work, the notation ‘‘+ h.c.’’ means ‘‘plus the Hermitian conjugate’’, like Lee et al. [21].

For example: $\Theta_{\mathbf{x}\mathcal{X}} \Theta_{\mathcal{X}\mathcal{X}}^{-1} k_{\mathcal{X}\mathbf{x}'} + h.c. = \Theta_{\mathbf{x}\mathcal{X}} \Theta_{\mathcal{X}\mathcal{X}}^{-1} k_{\mathcal{X}\mathbf{x}'} + \Theta_{\mathbf{x}'\mathcal{X}} \Theta_{\mathcal{X}\mathcal{X}}^{-1} k_{\mathcal{X}\mathbf{x}}$

²Up to a multiple of last layer width in standard parameterisation

on a test set \mathcal{X}' , in the infinite width limit. Note that Eq. (8) is the GP posterior using prior kernel Θ and noiseless observations $\tilde{f}_\infty(\mathcal{X})=\mathcal{Y}$, which we will refer to as the NTKGP posterior predictive. We construct \tilde{f} by sampling a random and untrainable function $\delta(\cdot)$ that is added to the standard forward pass $f(\cdot, \theta_t)$, defining an augmented forward pass:

$$\tilde{f}(\cdot, \theta_t) = f(\cdot, \theta_t) + \delta(\cdot) \quad (9)$$

Given a parameter initialisation scheme $\text{init}(\cdot)$ and initial parameters $\theta_0 \stackrel{d}{\sim} \text{init}(\cdot)$, our chosen formulation for $\delta(\cdot)$ is as follows: 1) sample $\tilde{\theta} \stackrel{d}{\sim} \text{init}(\cdot)$ independently of θ_0 ; 2) denote $\tilde{\theta} = \text{concat}(\{\tilde{\theta}^{\leq L}, \tilde{\theta}^{L+1}\})$; and 3) define $\theta^* = \text{concat}(\{\tilde{\theta}^{\leq L}, \mathbf{0}_{p_{L+1}}\})$. In words, we set the parameters in the final layer of an independently sampled $\tilde{\theta}$ to zero to obtain θ^* . Now, we define:

$$\delta(\mathbf{x}) = \nabla_{\theta} f(\mathbf{x}, \theta_0) \theta^* \quad (10)$$

There are a few important details to note about $\delta(\cdot)$ as defined in Eq. (10). First, $\delta(\cdot)$ has the same distribution in both NTK and standard parameterisations,³ and also $\delta(\cdot) | \theta_0 \stackrel{d}{\sim} \mathcal{GP}(0, \hat{\Theta}_0^{\leq L})$ in the NTK parameterisation.⁴ Moreover, Eq. (10) can be viewed as a single Jacobian-vector product (JVP), which packages that offer forward-mode autodifferentiation (AD), such as JAX [30], are reasonably efficient at computing for finite NNs. We chose this construction of \tilde{f} as it minimises computational and memory costs: alternatives are presented in Appendix C. The extra computational and memory costs of our methods, due to extra JVPs and parameter sets to store, are detailed in Appendix G.

To ascertain whether a trained \tilde{f}_∞ constructed via Eqs. (9, 10) returns a sample from the GP posterior Eq. (8) for wide NNs, the following proposition, which we prove in Appendix B.1, will be useful:

Proposition 1. $\delta(\cdot) \stackrel{d}{\sim} \mathcal{GP}(0, \Theta^{\leq L})$ and is independent of $f_0(\cdot)$ in the infinite width limit. Thus, $\tilde{f}_0(\cdot) = f_0(\cdot) + \delta(\cdot) \stackrel{d}{\sim} \mathcal{GP}(0, \Theta)$.

Using Proposition 1, we now consider the linearisation of $\tilde{f}_t(\cdot)$, noting that $\nabla_{\theta} \tilde{f}_0(\cdot) = \nabla_{\theta} f_0(\cdot)$:

$$\tilde{f}_t^{\text{lin}}(\mathbf{x}) = \underbrace{f_0(\mathbf{x}) + \nabla_{\theta^{L+1}} f(\mathbf{x}, \theta_0) \Delta \theta_t^{L+1}}_{\mathcal{K}} + \underbrace{\delta(\mathbf{x}) + \nabla_{\theta^{\leq L}} f(\mathbf{x}, \theta_0) \Delta \theta_t^{\leq L}}_{\Theta - \mathcal{K}} \quad (11)$$

The fact that $\nabla_{\theta} \tilde{f}_t^{\text{lin}}(\cdot) = \nabla_{\theta} f_0(\cdot)$ is crucial in Eq. (11), as this initial Jacobian is the feature map of the linearised NN regime from Lee et al. [21]. As per Proposition 1 and Eq. (11), we see that $\delta(\mathbf{x})$ adds the extra randomness missing from $f_0^{\text{lin}}(\mathbf{x})$ in Eq. (7), and reinitialises \tilde{f}_0 as a sample from $\mathcal{GP}(0, \mathcal{K})$ to $\mathcal{GP}(0, \Theta)$ for wide NNs. This means we can set $k = \Theta$ in Eq. (6) and deduce:

Corollary 1. $\tilde{f}_\infty(\mathcal{X}') \stackrel{d}{\sim} \mathcal{N}(\Theta_{\mathcal{X}'\mathcal{X}'} \Theta_{\mathcal{X}\mathcal{X}}^{-1} \mathcal{Y}, \Theta_{\mathcal{X}'\mathcal{X}'} - \Theta_{\mathcal{X}'\mathcal{X}} \Theta_{\mathcal{X}\mathcal{X}}^{-1} \Theta_{\mathcal{X}\mathcal{X}'})$, and hence a trained \tilde{f}_∞ returns a sample from the posterior NTKGP in the infinite width limit.

To summarise: we define our new NN forward pass to give $\tilde{f}_t(\mathbf{x}) = f_t(\mathbf{x}) + \delta(\mathbf{x})$ for standard forward pass $f_t(\mathbf{x})$, and an untrainable $\delta(\mathbf{x})$ defined as in Eq. (10). As given by Corollary 1, independently trained baselearners \tilde{f}_∞ can then be ensembled to approximate the NTKGP posterior predictive.

We will call \tilde{f}_∞ trained in this section an NTKGP baselearner, regardless of parameterisation or width. We are aware that the name NTK-GP has been used previously to refer to Eq. (6) with NNGP kernel \mathcal{K} , which is what standard training under squared error with a wide NN yields. However, we believe GPs in machine learning are synonymous with probabilistic inference [31], which Eq. (6) has no connection to in general, so we feel the name NTKGP is more appropriate for our methods.

³In this work Θ always denotes the NTK under NTK parameterisation. It is also possible to model Θ to be the scaled NTK under standard parameterisation (which depends on layer widths) as in Sohl-Dickstein et al. [28] with minor reweightings to both $\delta(\cdot)$ and, when modelling observation noise, the L^2 -regularisation described in Appendix D.

⁴With NTK parameterisation, it is easy to see that $\delta(\cdot) | \theta_0 \stackrel{d}{\sim} \mathcal{GP}(0, \hat{\Theta}_0^{\leq L})$, because $\tilde{\theta}^{\leq L} \stackrel{d}{\sim} \mathcal{N}(0, I_{p-p_{L+1}})$. To extend this to standard parameterisation, note that Eq. (10) is just the first order term in the Taylor expansion of $f(\mathbf{x}, \theta_0 + \theta^*)$, which has a parameterisation agnostic distribution, about θ_0 .

3.1 Modelling observation noise

So far, we have used squared loss $\ell(y, \tilde{f}(\mathbf{x}, \boldsymbol{\theta})) = \frac{1}{2\sigma^2}(y - \tilde{f}(\mathbf{x}, \boldsymbol{\theta}))^2$ for $\sigma^2=1$, and seen how our NTKGP training scheme for \tilde{f} gives a Bayesian interpretation to trained networks when we assume noiseless observations. Lemma 3 of Osband et al. [22] shows us how to draw a posterior sample for linear \tilde{f} if we wish to model Gaussian observation noise $y \stackrel{d}{\sim} \mathcal{N}(\tilde{f}(\mathbf{x}, \boldsymbol{\theta}), \sigma^2)$ for $\sigma^2>0$: by adding i.i.d. noise to targets $y'_n \stackrel{d}{\sim} \mathcal{N}(y_n, \sigma^2)$ and regularising $\mathcal{L}(\boldsymbol{\theta})$ with a weighted L^2 term, either $\|\boldsymbol{\theta}\|_{\Lambda}^2$ or $\|\boldsymbol{\theta} - \boldsymbol{\theta}_0\|_{\Lambda}^2$, depending on if you regularise in function space or parameter space. The weighting Λ will be detailed in Appendix D. These methods were introduced by Osband et al. [22] for the application of Q-learning in deep reinforcement learning, and are known as *Randomised Prior parameter* (RP-param) and *Randomised Prior function* (RP-fn) respectively. The randomised prior (RP) methods were motivated by a Bayesian linear regression approximation of the NN, but they do not take into account the difference between the NNGP and the NTK. Our NTKGP methods can be viewed as a way to fix this for both the parameter space or function space methods, which we will name NTKGP-param and NTKGP-fn respectively. Similar regularisation ideas were explored in connection to the NTK by Hu et al. [32], when the NN function is initialised from the origin, akin to kernel ridge regression.

3.2 Comparison of predictive distributions in infinite width

Having introduced the different ensemble training methods considered in this paper: NNGP; deep ensembles; randomised prior; and NTKGP, we will now compare their predictive distributions in the infinite width limit with squared error loss. Table 1 displays these limiting distributions, $f_{\infty}(\cdot) \stackrel{d}{\sim} \mathcal{GP}(\mu, \Sigma)$, and should be viewed as an extension to Equation (16) of Lee et al. [21].

Table 1: Predictive distributions of wide ensembles for various training methods. (std) denotes standard training with $f(\mathbf{x}, \boldsymbol{\theta})$, and (ours) denotes training using our additive $\delta(\mathbf{x})$ to make $\tilde{f}(\mathbf{x}, \boldsymbol{\theta})$.

Method	Layers trained	Output Noise	$\mu(\mathbf{x})$	$\Sigma(\mathbf{x}, \mathbf{x}')$
NNGP	Final	$\sigma^2 \geq 0$	$\mathcal{K}_{\mathbf{x}\mathcal{X}}(\mathcal{K}_{\mathcal{X}\mathcal{X}} + \sigma^2 I)^{-1}\mathcal{Y}$	$\mathcal{K}_{\mathbf{x}\mathbf{x}'} - \mathcal{K}_{\mathbf{x}\mathcal{X}}(\mathcal{K}_{\mathcal{X}\mathcal{X}} + \sigma^2 I)^{-1}\mathcal{K}_{\mathcal{X}\mathbf{x}'}$
Deep Ensembles	All (std)	$\sigma^2 = 0$	$\Theta_{\mathbf{x}\mathcal{X}}\Theta_{\mathcal{X}\mathcal{X}}^{-1}\mathcal{Y}$	$\mathcal{K}_{\mathbf{x}\mathbf{x}'} - (\Theta_{\mathbf{x}\mathcal{X}}\Theta_{\mathcal{X}\mathcal{X}}^{-1}\mathcal{K}_{\mathcal{X}\mathbf{x}'} + h.c.)$ $\Theta_{\mathbf{x}\mathcal{X}}\Theta_{\mathcal{X}\mathcal{X}}^{-1}\mathcal{K}_{\mathcal{X}\mathcal{X}}\Theta_{\mathcal{X}\mathcal{X}}^{-1}\Theta_{\mathcal{X}\mathbf{x}'}$
Randomised Prior	All (std)	$\sigma^2 > 0$	$\Theta_{\mathbf{x}\mathcal{X}}(\Theta_{\mathcal{X}\mathcal{X}} + \sigma^2 I)^{-1}\mathcal{Y}$	$\mathcal{K}_{\mathbf{x}\mathbf{x}'} - (\Theta_{\mathbf{x}\mathcal{X}}(\Theta_{\mathcal{X}\mathcal{X}} + \sigma^2 I)^{-1}\mathcal{K}_{\mathcal{X}\mathbf{x}'} + h.c.)$ $+ \Theta_{\mathbf{x}\mathcal{X}}(\Theta_{\mathcal{X}\mathcal{X}} + \sigma^2 I)^{-1}(\mathcal{K}_{\mathcal{X}\mathcal{X}} + \sigma^2 I)(\Theta_{\mathcal{X}\mathcal{X}} + \sigma^2 I)^{-1}\Theta_{\mathcal{X}\mathbf{x}'}$
NTKGP	All (ours)	$\sigma^2 \geq 0$	$\Theta_{\mathbf{x}\mathcal{X}}(\Theta_{\mathcal{X}\mathcal{X}} + \sigma^2 I)^{-1}\mathcal{Y}$	$\Theta_{\mathbf{x}\mathbf{x}'} - \Theta_{\mathbf{x}\mathcal{X}}(\Theta_{\mathcal{X}\mathcal{X}} + \sigma^2 I)^{-1}\Theta_{\mathcal{X}\mathbf{x}'}$

In order to parse Table 1, let us denote $\mu_{\text{NNGP}}, \mu_{\text{DE}}, \mu_{\text{RP}}, \mu_{\text{NTKGP}}$ and $\Sigma_{\text{NNGP}}, \Sigma_{\text{DE}}, \Sigma_{\text{RP}}, \Sigma_{\text{NTKGP}}$ to be the entries in the $\mu(\mathbf{x})$ and $\Sigma(\mathbf{x}, \mathbf{x}')$ columns of Table 1 respectively, read from top to bottom. We see that $\mu_{\text{DE}}(\mathbf{x}) = \mu_{\text{NTKGP}}(\mathbf{x})$ if $\sigma^2=0$, and $\mu_{\text{RP}}(\mathbf{x}) = \mu_{\text{NTKGP}}(\mathbf{x})$ if $\sigma^2>0$. In words: the predictive mean of a trained ensemble is the same when training all layers, both with standard training and our NTKGP training. This holds because both f_0 and \tilde{f}_0 are zero mean. It is also possible to compare the predictive covariances as the following proposition, proven in Appendix B.2, shows:

Proposition 2. For $\sigma^2=0$, $\Sigma_{\text{NTKGP}} \succeq \Sigma_{\text{DE}} \succeq \Sigma_{\text{NNGP}}$. Similarly, for $\sigma^2>0$, $\Sigma_{\text{NTKGP}} \succeq \Sigma_{\text{RP}} \succeq \Sigma_{\text{NNGP}}$.

Here, when we write $k_1 \succeq k_2$ for p.d. kernels k_1, k_2 , we mean that $k_1 - k_2$ is also a p.d. kernel. One consequence of Proposition 2 is that the predictive distribution of an ensemble of NNs trained via our NTKGP methods is always more conservative than a standard deep ensemble, in the linearised NN regime, when the ensemble size $K \rightarrow \infty$. It is not possible to say in general when this will be beneficial, because in practice our models will always be misspecified. However, Proposition 2 suggests that in situations where we suspect standard deep ensembles might be overconfident, such as in situations where we expect some dataset shift at test time, our methods should hold an advantage.

3.3 Modelling heteroscedasticity

Following Lakshminarayanan et al. [11], if we wish to model heteroscedasticity in a univariate regression setting such that each training point, (\mathbf{x}_n, y_n) , has an individual observation noise $\sigma^2(\mathbf{x}_n)$ then we use the heteroscedastic Gaussian NLL loss (up to additive constant):

$$\ell(y'_n, \tilde{f}(\mathbf{x}_n, \boldsymbol{\theta})) = \frac{(y'_n - \tilde{f}(\mathbf{x}_n, \boldsymbol{\theta}))^2}{2\sigma^2(\mathbf{x}_n)} + \frac{\log \sigma^2(\mathbf{x}_n)}{2} \quad (12)$$

where $y'_n = y_n + \sigma(\mathbf{x}_n)\epsilon_n$ and $\epsilon_n \stackrel{\text{i.i.d.}}{\sim} \mathcal{N}(0, 1)$. It is easy to see that for fixed $\sigma^2(\mathbf{x}_n)$, our NTKGP trained baselearners will still have a Bayesian interpretation: $\mathcal{Y}' \leftarrow \Sigma^{-\frac{1}{2}}\mathcal{Y}'$ and $\tilde{f}(\mathcal{X}, \boldsymbol{\theta}) \leftarrow \Sigma^{-\frac{1}{2}}\tilde{f}(\mathcal{X}, \boldsymbol{\theta})$ returns us to the homoscedastic case, where $\Sigma = \text{diag}(\sigma^2(\mathcal{X})) \in \mathbb{R}^{N \times N}$. We will follow Lakshminarayanan et al. [11] and parameterise $\sigma^2(\mathbf{x}) = \sigma_{\theta}^2(\mathbf{x})$ by an extra output head of the NN, that is trainable alongside the mean function $\mu_{\theta}(\mathbf{x})$ when modelling heteroscedasticity.⁵

3.4 NTKGP Ensemble Algorithms

We now proceed to train an ensemble of K NTKGP baselearners. Like previous work [11, 22], we independently initialise baselearners, and also use a fixed, independently sampled training set noise $\epsilon_k \in \mathbb{R}^{N^C}$ if modelling output noise. These implementation details are all designed to encourage diversity among baselearners, with the goal of approximating the NTKGP posterior predictive for our Bayesian deep ensembles. Appendix F details how to aggregate predictions from trained baselearners. In Algorithm 1, we outline our NTKGP-param method: `data_noise` adds observation noise to targets; `concat` denotes a concatenation operation; and `init(·)` will be standard parameterisation initialisation in the JAX library Neural Tangents [33] unless stated otherwise. As discussed by Pearce et al. [23], there is a choice between ‘‘anchoring’’/regularising parameters towards their initialisation or an independently sampled parameter set when modelling observation noise. We anchor at initialisation as the linearised NN regime only holds local to parameter initialisation [21], and also this reduces the memory cost of sampling parameters sets. Appendix E details our NTKGP-fn method.

Algorithm 1 NTKGP-param ensemble

Require: Data $\mathcal{D} = \{\mathcal{X}, \mathcal{Y}\}$, loss function \mathcal{L} , NN model $f_{\theta} : \mathcal{X} \rightarrow \mathcal{Y}$, Ensemble size $K \in \mathbb{N}$, noise procedure: `data_noise`, NN parameter initialisation scheme: `init(·)`

for $k = 1, \dots, K$ **do**

Form $\{\mathcal{X}_k, \mathcal{Y}_k\} = \text{data_noise}(\mathcal{D})$

Initialise $\boldsymbol{\theta}_k \stackrel{d}{\sim} \text{init}(\cdot)$

Initialise $\tilde{\boldsymbol{\theta}}_k \stackrel{d}{\sim} \text{init}(\cdot)$ and denote $\tilde{\boldsymbol{\theta}}_k = \text{concat}(\{\tilde{\boldsymbol{\theta}}_k^{\leq L}, \tilde{\boldsymbol{\theta}}_k^{L+1}\})$

Set $\boldsymbol{\theta}_k^* = \text{concat}(\{\tilde{\boldsymbol{\theta}}_k^{\leq L}, \mathbf{0}_{p_{L+1}}\})$

Define $\delta(\mathbf{x}) = \nabla_{\boldsymbol{\theta}} f(\mathbf{x}, \boldsymbol{\theta}_k^*) \boldsymbol{\theta}_k^*$

Define $\tilde{f}_k(\mathbf{x}, \boldsymbol{\theta}_t) = f(\mathbf{x}, \boldsymbol{\theta}_t) + \delta(\mathbf{x})$ and set $\boldsymbol{\theta}_0 = \boldsymbol{\theta}_k$

Optimise $\mathcal{L}(\tilde{f}_k(\mathcal{X}_k, \boldsymbol{\theta}_t), \mathcal{Y}_k) + \frac{1}{2} \|\boldsymbol{\theta}_t - \boldsymbol{\theta}_k\|_{\Lambda}^2$ for $\boldsymbol{\theta}_t$ to obtain $\hat{\boldsymbol{\theta}}_k$

end for

return ensemble $\{\tilde{f}_k(\cdot, \hat{\boldsymbol{\theta}}_k)\}_{k=1}^K$

3.5 Classification methodology

For classification tasks with a non-linear link function, such as softmax, it is possible to apply our methods with observation noise as described in Algorithm 1 in order to obtain a Laplace approximation interpretation to our trained ensemble. A similar approach has been considered for a single NN by Khan et al. [34], but there the authors consider the empirical NTK at a trained $\hat{\boldsymbol{\theta}}$ instead of at initialisation. Empirically, we found output noise in classification tasks to degrade performance for NNs. Instead, we forgo observation noise and add a small amount of label smoothing [35] as regularisation, alongside softmax link function. There is still a posterior interpretation to our methods,

⁵We use the *sigmoid* function, instead of *softplus* [11], to enforce positivity on $\sigma_{\theta}^2(\cdot)$, because our data will be standardised.

by treating the label-smoothed target logits as regression targets. Previous NTK applications to classification tasks [21, 36] have considered using a linear link function with squared error loss, but this does not give probabilistic predictions and is therefore not appropriate for our methods.

4 Experiments

Due to limited space, Appendix H will contain all experimental details not discussed in this section.

Toy 1D regression task We begin with a toy 1D example $y = x\sin(x) + \epsilon$, using homoscedastic $\epsilon \stackrel{d}{\sim} \mathcal{N}(0, 0.1^2)$. We use a training set of 20 points partitioned into two clusters, in order to detail uncertainty on out-of-distribution test data. For each ensemble method, we use MLP baselearners with two hidden layers of width 512, and erf activation. The choice of erf activation means that both the NTK Θ and NNGP kernel \mathcal{K} are analytically available [21, 37]. We can compare ensemble methods to the analytic GP posterior using either Θ or \mathcal{K} as prior covariance function via the Neural Tangents library [33], with only slight modifications to the existing library at the time of writing.

Figure 1 compares the analytic NTKGP posterior predictive with the analytic NNGP posterior predictive, as well as three different ensemble methods: deep ensembles, RP-param and NTKGP-param. We plot 95% predictive confidence intervals, treating ensembles as one Gaussian predictive distribution with matched moments like Lakshminarayanan et al. [11]. As expected, both NTKGP-param and RP-param ensembles have similar predictive means to the analytic NTKGP posterior. Likewise, we see that only our NTKGP-param ensemble predictive variances match the analytic NTKGP posterior. As foreseen in Proposition 2, the analytic NNGP posterior and other ensemble methods make more confident predictions than the NTKGP posterior, which in this example results in overconfidence on out-of-distribution data.⁶

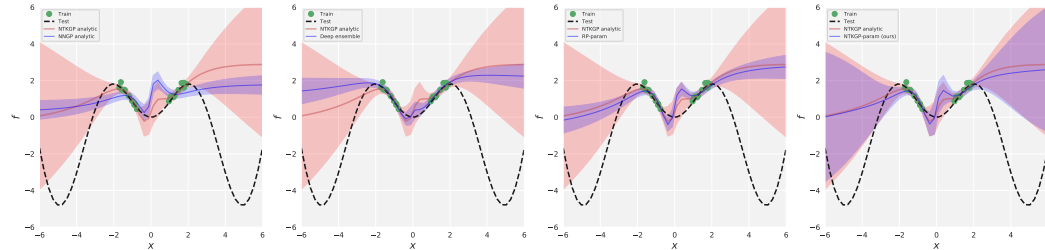


Figure 1: All subplots plot the analytic NTKGP posterior (in red). From left to right, (in blue): analytic NNGP posterior; deep ensembles; RP-param; and NTKGP-param (ours). For each method we plot the mean prediction and 95% predictive confidence interval. Green points denote the training data, and the black dotted line is the true test function $y = x\sin(x)$.

Flight Delays We now compare different ensemble methods on a large scale regression problem using the Flight Delays dataset [38], which is known to contain dataset shift. We train heteroscedastic baselearners on the first 700k data points and test on the next 100k test points at 5 different starting points: 700k, 2m (million), 3m, 4m and 5m. The dataset is ordered chronologically in date through the year 2008, so we expect the NTKGP methods to outperform standard deep ensembles for the later starting points. Figure 2 (Left) confirms our hypothesis. Interestingly, there seems to be a seasonal effect between the 3m and 4m test set that results in stronger performance in the 4m test set than the 3m test set, for ensembles trained on the first 700k data points. We see that our Bayesian deep ensembles perform slightly worse than standard deep ensembles when there is little or no test data shift, but fail more gracefully as the level of dataset shift increases.

Figure 2 (Right) plots confidence versus error for different ensemble methods on the combined test set of $5 \times 100k$ points. For each precision threshold τ , we plot root-mean-squared error (RMSE) on examples where predictive precision is larger than τ , indicating confidence. As we can see, our NTKGP methods incur lower error over all precision thresholds, and this contrast in performance is magnified for more confident predictions.

⁶Code for this experiment is available at: <https://github.com/bobby-he/bayesian-ntk>.

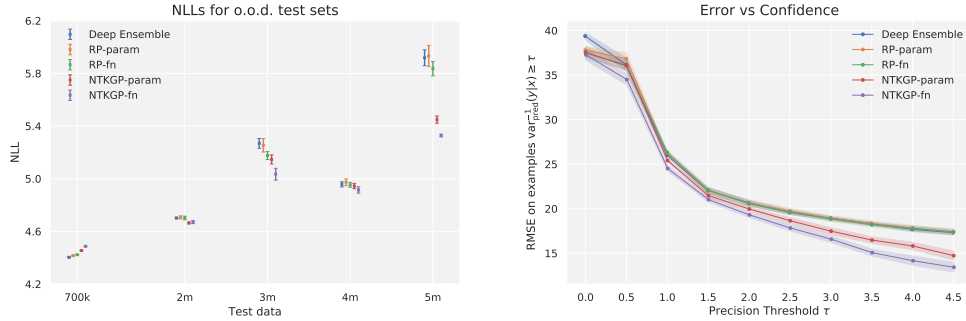


Figure 2: (Left) Flight Delays NLLs for ensemble methods trained on first 700k points of the dataset and tested on various out-of-distribution test sets, with time shift between training set and test set increasing along the x -axis. (Right) Error vs Confidence curves for ensembles tested on all $5 \times 100k$ test points combined. Both plots include 95% CIs corresponding to 10 independent ensembles.

MNIST vs NotMNIST We next move onto classification experiments, comparing ensembles trained on MNIST and tested on both MNIST and NotMNIST.⁷ First, we verify that underconfidence is not impairing our methods on in-distribution MNIST test set classification performance: Figure 3 (Left) confirms this is the case across various ensemble sizes. For each ensemble size, we plot 95% confidence intervals for the mean classification accuracy, across 10 independently trained ensembles.

Finally, Figure 3 (Right) depicts the error versus confidence plot of different ensemble methods trained on MNIST and tested on both MNIST and NotMNIST. For each test point (x, y) , we calculate the ensemble prediction $p(y = k|\mathbf{x})$ and define the predicted label as $\hat{y} = \operatorname{argmax}_k p(y = k|\mathbf{x})$, with confidence $p(y = \hat{y}|\mathbf{x})$. Like Lakshminarayanan et al. [11], for each confidence threshold $0 \leq \tau \leq 1$, we plot the average error for all test points that are more confident than τ . We count all predictions on the NotMNIST test set to be incorrect. We see in Figure 3 (Right) that the NTKGP methods significantly outperform both deep ensembles and RP-fn. This is because our methods make more conservative predictions on the out-of-distribution NotMNIST test set, as can be seen by Figure 4 in Appendix H, which plots histograms of predictive entropies.

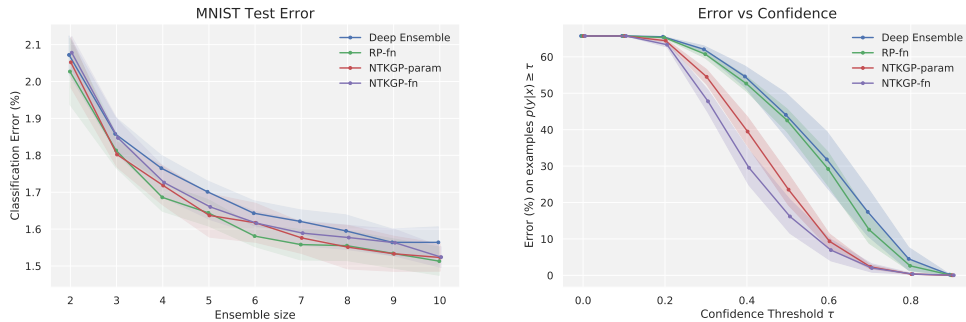


Figure 3: (Left) Classification error on MNIST test set for different ensemble sizes. (Right) Error versus Confidence plots of ensembles trained on MNIST and tested on both MNIST and NotMNIST. Both plots include 95% CIs corresponding to 10 independent ensembles.

5 Discussion

We built on existing work regarding the Neural Tangent Kernel (NTK), which showed that there is no posterior predictive interpretation to a standard deep ensemble in the infinite width limit. We introduced a simple modification to training that enables a GP posterior predictive interpretation for a wide ensemble, and showed empirically that our Bayesian deep ensembles emulate the analytic posterior predictive when it is available. In addition, we demonstrated that our Bayesian deep ensembles outperform standard deep ensembles in out-of-distribution settings for both regression and classification tasks.

⁷Available at <http://yaroslavvb.blogspot.com/2011/09/notmnist-dataset.html>

Our work has several limitations. First, though we have tried to minimise additional computational costs, our ensembles are at best as expensive as standard deep ensembles, and may perform worse than standard deep ensembles when confident predictions are not detrimental. Moreover, our analyses are firmly planted in the “lazy learning” regime [39], with no consideration for finite width corrections to the NTK during training, nor provision of quantitative results relating NN width to the NTKGP posterior approximation.

In future work, we would like to apply our Bayesian deep ensembles to deeper NN architectures. A natural question that emerges is how to tune hyperparameters of the NTK to best capture inductive biases or prior beliefs about the data. Possible lines of enquiry include: the large-depth limit [40], the choice of architecture [41], and the choice of activation [42]. Finally, we would like to assess our Bayesian deep ensembles in non-supervised learning settings, such as active learning or reinforcement learning.

Acknowledgments and Disclosure of Funding

We thank Arnaud Doucet, Edwin Fong, Michael Hutchinson, Lewis Smith, Jasper Snoek, Jascha Sohl-Dickstein and Sheheryar Zaidi for helpful discussions and feedback. We also thank the JAX and Neural Tangents teams for their open-source software. BH is supported by the EPSRC and MRC through the OxWaSP CDT programme (EP/L016710/1).

References

- [1] James Aitchison. Goodness of Prediction Fit. *Biometrika*, 62(3):547–554, 1975.
- [2] David JC MacKay. *Bayesian Methods for Adaptive Models*. PhD thesis, California Institute of Technology, 1992.
- [3] Radford M Neal. *Bayesian Learning for Neural Networks*, volume 118. Springer Science & Business Media, 2012.
- [4] Max Welling and Yee W Teh. Bayesian Learning via Stochastic Gradient Langevin Dynamics. In *Proceedings of the 28th International Conference on Machine Learning (ICML-11)*, pages 681–688, 2011.
- [5] Alex Graves. Practical Variational Inference for Neural Networks. In *Advances in Neural Information Processing Systems*, pages 2348–2356, 2011.
- [6] Charles Blundell, Julien Cornebise, Koray Kavukcuoglu, and Daan Wierstra. Weight Uncertainty in Neural Networks. In *International Conference on Machine Learning*, pages 1613–1622, 2015.
- [7] Christos Louizos and Max Welling. Multiplicative Normalizing Flows for Variational Bayesian Neural Networks. In *Proceedings of the 34th International Conference on Machine Learning - Volume 70*, pages 2218–2227. JMLR. org, 2017.
- [8] Yeming Wen, Paul Vicol, Jimmy Ba, Dustin Tran, and Roger Grosse. Flipout: Efficient Pseudo-Independent Weight Perturbations on Mini-Batches. *arXiv preprint arXiv:1803.04386*, 2018.
- [9] Shengyang Sun, Guodong Zhang, Jiaxin Shi, and Roger Grosse. Functional Variational Bayesian Neural Networks. *arXiv preprint arXiv:1903.05779*, 2019.
- [10] Yarin Gal and Zoubin Ghahramani. Dropout as a Bayesian Approximation: Representing Model Uncertainty in Deep Learning. In *International Conference on Machine Learning*, pages 1050–1059, 2016.
- [11] Balaji Lakshminarayanan, Alexander Pritzel, and Charles Blundell. Simple and Scalable Predictive Uncertainty Estimation using Deep Ensembles. In *Advances in Neural Information Processing Systems*, pages 6402–6413, 2017.

- [12] Yaniv Ovadia, Emily Fertig, Jie Ren, Zachary Nado, D Sculley, Sebastian Nowozin, Joshua V Dillion, Balaji Lakshminarayanan, and Jasper Snoek. Can You Trust Your Model’s Uncertainty? Evaluating Predictive Uncertainty Under Dataset Shift. In *NeurIPS*, 2019.
- [13] Stanislav Fort, Huiyi Hu, and Balaji Lakshminarayanan. Deep Ensembles: A Loss Landscape Perspective. *arXiv preprint arXiv:1912.02757*, 2019.
- [14] Andrew Gordon Wilson and Pavel Izmailov. Bayesian Deep Learning and a Probabilistic Perspective of Generalization. *arXiv preprint arXiv:2002.08791*, 2020.
- [15] Radford M Neal. Priors for Infinite Networks. In *Bayesian Learning for Neural Networks*, pages 29–53. Springer, 1996.
- [16] Jaehoon Lee, Jascha Sohl-dickstein, Jeffrey Pennington, Roman Novak, Sam Schoenholz, and Yasaman Bahri. Deep Neural Networks as Gaussian Processes. In *International Conference on Learning Representations*, 2018.
- [17] Alexander G de G Matthews, Mark Rowland, Jiri Hron, Richard E Turner, and Zoubin Ghahramani. Gaussian Process Behaviour in Wide Deep Neural Networks. In *International Conference on Learning Representations*, volume 4, 2018.
- [18] Adrià Garriga-Alonso, Carl Edward Rasmussen, and Laurence Aitchison. Deep Convolutional Networks as shallow Gaussian Processes. In *International Conference on Learning Representations*, 2019.
- [19] Roman Novak, Lechao Xiao, Yasaman Bahri, Jaehoon Lee, Greg Yang, Daniel A. Abolafia, Jeffrey Pennington, and Jascha Sohl-dickstein. Bayesian Deep Convolutional Networks with Many Channels are Gaussian Processes. In *International Conference on Learning Representations*, 2019.
- [20] Arthur Jacot, Franck Gabriel, and Clément Hongler. Neural Tangent Kernel: Convergence and Generalization in Neural Networks. In *Advances in Neural Information Processing Systems*, pages 8571–8580, 2018.
- [21] Jaehoon Lee, Lechao Xiao, Samuel Schoenholz, Yasaman Bahri, Roman Novak, Jascha Sohl-Dickstein, and Jeffrey Pennington. Wide Neural Networks of Any Depth Evolve as Linear Models under gradient descent. In *Advances in Neural Information Processing Systems*, pages 8570–8581, 2019.
- [22] Ian Osband, John Aslanides, and Albin Cassirer. Randomized Prior Functions for Deep Reinforcement Learning. In *Advances in Neural Information Processing Systems*, pages 8617–8629, 2018.
- [23] Tim Pearce, Mohamed Zaki, Alexandra Brintrup, Nicolas Anastassacos, and Andy Neely. Uncertainty in Neural Networks: Bayesian Ensembling. *arXiv preprint arXiv:1810.05546*, 2018.
- [24] Yehuda Hoffman and Erez Ribak. Constrained Realizations of Gaussian Fields: A Simple Algorithm. *The Astrophysical Journal*, 380:L5–L8, 1991.
- [25] Greg Yang. Scaling Limits of Wide Neural Networks with Weight Sharing: Gaussian Process Behavior, Gradient Independence, and Neural Tangent Kernel Derivation. *arXiv preprint arXiv:1902.04760*, 2019.
- [26] Ryo Karakida, Shotaro Akaho, and Shun-ichi Amari. Universal Statistics of Fisher Information in Deep Neural Networks: Mean Field Approach. In *The 22nd International Conference on Artificial Intelligence and Statistics*, pages 1032–1041, 2019.
- [27] Daniel Park, Jascha Sohl-Dickstein, Quoc Le, and Samuel Smith. The Effect of Network Width on Stochastic Gradient Descent and Generalization: an Empirical Study. In *International Conference on Machine Learning*, pages 5042–5051, 2019.
- [28] Jascha Sohl-Dickstein, Roman Novak, Samuel S Schoenholz, and Jaehoon Lee. On the infinite width limit of neural networks with a standard parameterization. *arXiv preprint arXiv:2001.07301*, 2020.

- [29] Alexander G de G Matthews, Jiri Hron, Richard E Turner, and Zoubin Ghahramani. Sample-then-optimize posterior sampling for Bayesian linear models. In *NeurIPS Workshop on Advances in Approximate Bayesian Inference*, 2017.
- [30] James Bradbury, Roy Frostig, Peter Hawkins, Matthew James Johnson, Chris Leary, Dougal Maclaurin, and Skye Wanderman-Milne. JAX: composable transformations of Python+NumPy programs, 2018. URL <http://github.com/google/jax>.
- [31] Carl Edward Rasmussen. Gaussian Processes in Machine Learning. In *Summer School on Machine Learning*, pages 63–71. Springer, 2003.
- [32] Wei Hu, Zhiyuan Li, and Dingli Yu. Simple and Effective Regularization Methods for Training on Noisily Labeled Data with Generalization Guarantee. In *International Conference on Learning Representations*, 2020. URL <https://openreview.net/forum?id=Hke3gyHYwH>.
- [33] Roman Novak, Lechao Xiao, Jiri Hron, Jaehoon Lee, Alexander A. Alemi, Jascha Sohl-Dickstein, and Samuel S. Schoenholz. Neural Tangents: Fast and Easy Infinite Neural Networks in Python. In *International Conference on Learning Representations*, 2020. URL <https://github.com/google/neural-tangents>.
- [34] Mohammad Emtiyaz E Khan, Alexander Immer, Ehsan Abedi, and Maciej Korzepa. Approximate Inference Turns Deep Networks into Gaussian Processes. In *Advances in Neural Information Processing Systems*, pages 3088–3098, 2019.
- [35] Gabriel Pereyra, George Tucker, Jan Chorowski, Łukasz Kaiser, and Geoffrey Hinton. Regularizing Neural Networks by Penalizing Confident Output Distributions. *arXiv preprint arXiv:1701.06548*, 2017.
- [36] Sanjeev Arora, Simon S Du, Wei Hu, Zhiyuan Li, Russ R Salakhutdinov, and Ruosong Wang. On Exact Computation with an Infinitely Wide Neural Net. In *Advances in Neural Information Processing Systems*, pages 8139–8148, 2019.
- [37] Christopher KI Williams. Computing with Infinite Networks. In *Advances in neural information processing systems*, pages 295–301, 1997.
- [38] James Hensman, Nicolo Fusi, and Neil D Lawrence. Gaussian Processes for Big Data. In *Uncertainty in Artificial Intelligence*, page 282. Citeseer, 2013.
- [39] Lenaic Chizat, Edouard Oyallon, and Francis Bach. On Lazy Training in Differentiable Programming. In *Advances in Neural Information Processing Systems*, pages 2937–2947, 2019.
- [40] Soufiane Hayou, Arnaud Doucet, and Judith Rousseau. Mean-field Behaviour of Neural Tangent Kernel for Deep Neural Networks. *arXiv preprint arXiv:1905.13654*, 2019.
- [41] Sheheryar Zaidi, Arber Zela, Thomas Elsken, Chris Holmes, Frank Hutter, and Yee Whye Teh. Neural Ensemble Search for Performant and Calibrated Predictions, 2020.
- [42] Matthew Tancik, Pratul P Srinivasan, Ben Mildenhall, Sara Fridovich-Keil, Nithin Raghavan, Utkarsh Singhal, Ravi Ramamoorthi, Jonathan T Barron, and Ren Ng. Fourier Features Let Networks Learn High Frequency Functions in Low Dimensional Domains. *arXiv preprint arXiv:2006.10739*, 2020.
- [43] Yann A LeCun, Léon Bottou, Genevieve B Orr, and Klaus-Robert Müller. Efficient BackProp. In *Neural networks: Tricks of the trade*, pages 9–48. Springer, 2012.
- [44] Kaiming He, Xiangyu Zhang, Shaoqing Ren, and Jian Sun. Delving Deep into Rectifiers: Surpassing Human-Level Performance on Imagenet Classification. In *The IEEE International Conference on Computer Vision (ICCV)*, December 2015.
- [45] David Williams. *Probability with Martingales*. Cambridge University Press, 1991. doi: 10.1017/CBO9780511813658.
- [46] Harald Cramér and Herman Wold. Some Theorems on Distribution Functions. *Journal of the London Mathematical Society*, 1(4):290–294, 1936.

- [47] Patrick Billingsley. *Probability and Measure*. John Wiley and Sons, second edition, 1986.
- [48] Joost van Amersfoort, Lewis Smith, Yee Whye Teh, and Yarin Gal. Simple and Scalable Epistemic Uncertainty Estimation Using a Single Deep Deterministic Neural Network, 2020.
- [49] Diederik P Kingma and Jimmy Ba. Adam: A Method for Stochastic Optimization. *arXiv preprint arXiv:1412.6980*, 2014.
- [50] E Fong and C C Holmes. On the marginal likelihood and cross-validation. *Biometrika*, 107(2):489–496, 01 2020. ISSN 0006-3444. doi: 10.1093/biomet/asz077. URL <https://doi.org/10.1093/biomet/asz077>.

A Recap of standard and NTK parameterisations

For completeness, we recap the difference between standard and NTK parameterisations & initialisations [20, 21] for an MLP in this section.

Consider an MLP with L hidden layers of widths from $n_0=d$ to n_L respectively, and final readout layer with $n_{L+1} = C$. For a given $\mathbf{x} \in \mathbb{R}^d$, under the NTK parameterisation the recurrence relation that constitutes the forward pass of the NN is then:

$$\alpha^{(0)}(\mathbf{x}, \boldsymbol{\theta}) = \mathbf{x} \quad (13)$$

$$\tilde{\alpha}^{(l+1)}(\mathbf{x}, \boldsymbol{\theta}) = \frac{\sigma_W}{\sqrt{n_l}} W^{(l)} \alpha^{(l)}(\mathbf{x}, \boldsymbol{\theta}) + \sigma_b b^{(l)} \quad (14)$$

$$\alpha^{(l)}(\mathbf{x}, \boldsymbol{\theta}) = \phi(\tilde{\alpha}^{(l)}(\mathbf{x}, \boldsymbol{\theta})) \quad (15)$$

for $l \leq L$ where $\tilde{\alpha}^{(l)}$ and $\alpha^{(l)}$ are the preactivations and activations respectively at layer l , with entrywise nonlinearity $\phi(\cdot)$. In the NTK parameterisation, all parameters $W^{(l)} \in \mathbb{R}^{n_{l+1} \times n_l}$ and $b^{(l)} \in \mathbb{R}^{n_{l+1}}$ for all layers l are initialised as i.i.d. standard normal $\mathcal{N}(0, 1)$. The hyperparameters σ_W and σ_b are known as the weight and bias variances respectively, and are hyperparameters of the infinite width limit NTK Θ .

On the other hand, under *standard* parameterisation, the recurrence relation of the NN is:

$$\alpha^{(0)}(\mathbf{x}, \boldsymbol{\theta}) = \mathbf{x} \quad (16)$$

$$\tilde{\alpha}^{(l+1)}(\mathbf{x}, \boldsymbol{\theta}) = W^{(l)} \alpha^{(l)}(\mathbf{x}, \boldsymbol{\theta}) + b^{(l)} \quad (17)$$

$$\alpha^{(l)}(\mathbf{x}, \boldsymbol{\theta}) = \phi(\tilde{\alpha}^{(l)}(\mathbf{x}, \boldsymbol{\theta})) \quad (18)$$

with $W_{i,j}^{(l)} \sim \mathcal{N}(0, \frac{1}{n_l} \sigma_W^2)$ and $b_j^{(l)} \sim \mathcal{N}(0, \sigma_b^2)$ at initialisation. Commonly used initialisation schemes like LeCun [43] or He [44] fall into this category.

Regardless of parameterisation, our notation from Sections 2 & 3 corresponds to $f(\mathbf{x}, \boldsymbol{\theta}) = \tilde{\alpha}^{(L+1)}(\mathbf{x}, \boldsymbol{\theta})$, with $\boldsymbol{\theta} = \{W^{(l)}, b^{(l)}\}_{l=0}^L$, $\boldsymbol{\theta}^{\leq L} = \{W^{(l)}, b^{(l)}\}_{l=0}^{L-1}$ and $\boldsymbol{\theta}^{L+1} = \{W^{(L)}, b^{(L)}\}$.

We see that the different parameterisations yield the same distribution for the functional output $f(\cdot, \boldsymbol{\theta})$ at initialisation, but give different scalings to the parameter gradients in the backward pass. Sohl-Dickstein et al. [28] have recently explored further variants of these parameterisations.

B Proofs

B.1 Proof of Proposition 1

Proposition 3 (Proposition 1 restated). $\delta(\cdot) \xrightarrow{d} \mathcal{GP}(0, \Theta^{\leq L})$ and is independent of $f_0(\cdot)$ in the infinite width limit. Thus, $\tilde{f}_0(\cdot) = f_0(\cdot) + \delta(\cdot) \xrightarrow{d} \mathcal{GP}(0, \Theta)$.

Proof. For notational ease, let us define two jointly independent GPs $g(\cdot) \stackrel{d}{\sim} \mathcal{GP}(0, \Theta^{\leq L})$ & $h(\cdot) \stackrel{d}{\sim} \mathcal{GP}(0, \mathcal{K})$. By independence, we have $g(\cdot) + h(\cdot) \stackrel{d}{\sim} \mathcal{GP}(0, \Theta)$. Moreover, let $\delta_m(\cdot), f_m^0(\cdot)$ and $\boldsymbol{\theta}_m^0$ denote $\delta(\cdot), f_0(\cdot)$ and $\boldsymbol{\theta}_0$ respectively at width parameter $m \in \mathbb{N}$. The infinite width limit thus corresponds to $m \rightarrow \infty$.

For our purposes, it will be sufficient to prove convergence of finite-dimensional marginals, $(\delta_m(\mathcal{X}), f_m^0(\mathcal{X}')) \xrightarrow{d} (g(\mathcal{X}), h(\mathcal{X}'))$ jointly, for arbitrary sets of inputs $\mathcal{X}, \mathcal{X}'$. Note that previous work [16, 17] has already shown that $f_m^0(\mathcal{X}') \xrightarrow{d} h(\mathcal{X}')$.

The proof that $(\delta_m(\mathcal{X}), f_m^0(\mathcal{X}')) \xrightarrow{d} (g(\mathcal{X}), h(\mathcal{X}'))$ relies on Lévy's Convergence theorem [45] and the Cramér-Wold device [46, 47]. Using these results it is sufficient to show, denoting φ_X as the characteristic function of a random variable X , that:

$$\varphi_{Y_m}(t) \rightarrow \varphi_Y(t) \quad (19)$$

where $Y_m = u^\top \delta_m(\mathcal{X}) + v^\top f_m^0(\mathcal{X}')$ and $Y = u^\top g(\mathcal{X}) + v^\top h(\mathcal{X}')$, for all $t \in \mathbb{R}$, $u \in \mathbb{R}^{|\mathcal{X}|C}$ and $v \in \mathbb{R}^{|\mathcal{X}'|C}$. But:

$$\varphi_{Y_m}(t) = \mathbb{E}[\exp(itY_m)] \quad (20)$$

$$= \mathbb{E}\left[\mathbb{E}[\exp(itY_m) \mid \theta_{0,m}]\right] \quad (21)$$

$$= \mathbb{E}_{\theta_{0,m}}[\exp(-t^2 u^\top \hat{\Theta}_{0,m}^{\leq L}(\mathcal{X}, \mathcal{X})u + itv^\top f_m^0(\mathcal{X}'))] \quad (22)$$

$$= \exp(-t^2 u^\top \Theta^{\leq L}(\mathcal{X}, \mathcal{X})u) \mathbb{E}_{\theta_{0,m}}[\exp(itv^\top f_m^0(\mathcal{X}'))] + r_m \quad (23)$$

$$\rightarrow \mathbb{E}[\exp(itY)] \quad (24)$$

where r_m , defined as the difference between Eqs. (23) & (22), can be shown to be $o_m(1)$ using the Bounded Convergence theorem and the empirical NTK convergence results, and by noting that proofs of NTK convergence [20, 21, 25] are all done on a layer-by-layer basis.

The claim that $\tilde{f}_0(\cdot) = f_0(\cdot) + \delta(x) \xrightarrow{d} \mathcal{GP}(0, \Theta)$ then follows by setting $\mathcal{X} = \mathcal{X}'$ and $v = u$. □

B.2 Proof of Proposition 2

Proposition 4 (Proposition 2 restated). *We have $\Sigma_{NTKGP} \succeq \Sigma_{DE} \succeq \Sigma_{NNGP}$ for $\sigma^2 = 0$. Similarly, for $\sigma^2 > 0$, we have $\Sigma_{NTKGP} \succeq \Sigma_{RP} \succeq \Sigma_{NNGP}$.*

Proof. We will prove the case for $\sigma^2 > 0$ as the case for $\sigma^2 = 0$ is similar, and one can replace inversions of $\Theta(\mathcal{X}, \mathcal{X})$ and $\mathcal{K}(\mathcal{X}, \mathcal{X})$ with generalised inverses if need be.

Let \mathcal{X}' be an arbitrary test set. We will first show $\Sigma_{RP} \succeq \Sigma_{NNGP}$. It will suffice to show that $\Sigma_{RP}(\mathcal{X}', \mathcal{X}') - \Sigma_{NNGP}(\mathcal{X}', \mathcal{X}') \succeq 0$ is a p.s.d. matrix. But it is not hard to check that:

$$\Sigma_{RP}(\mathcal{X}', \mathcal{X}') - \Sigma_{NNGP}(\mathcal{X}', \mathcal{X}') = U(\mathcal{K}(\mathcal{X}, \mathcal{X}) + \sigma^2 I)U^\top \quad (25)$$

which is clearly p.s.d, where $U = \Theta(\mathcal{X}', \mathcal{X}')(\Theta(\mathcal{X}, \mathcal{X}) + \sigma^2 I)^{-1} - \mathcal{K}(\mathcal{X}', \mathcal{X}')(\mathcal{K}(\mathcal{X}, \mathcal{X}) + \sigma^2 I)^{-1} \in \mathbb{R}^{|\mathcal{X}'| \times |\mathcal{X}'|}$

Likewise, to show $\Sigma_{NTK} \succeq \Sigma_{RP}$ we can check that:

$$\Sigma_{NTK}(\mathcal{X}', \mathcal{X}') - \Sigma_{RP}(\mathcal{X}', \mathcal{X}') = U_1 + U_2 \Delta(\mathcal{X}, \mathcal{X}) U_2^\top \succeq 0 \quad (26)$$

where

$$U_1 = \Delta(\mathcal{X}', \mathcal{X}') - \Delta(\mathcal{X}', \mathcal{X}) \Delta^g(\mathcal{X}, \mathcal{X}) \Delta(\mathcal{X}, \mathcal{X}') \quad (27)$$

and $\Delta = \Theta^{\leq L} \succeq 0$ is the contributions to the NTK from parameters before the final layer as before. Finally, we need to define U_2 as:

$$U_2 = \Theta(\mathcal{X}', \mathcal{X}')(\Theta(\mathcal{X}, \mathcal{X}) + \sigma^2 I)^{-1} - \Delta(\mathcal{X}', \mathcal{X}) \Delta^g(\mathcal{X}, \mathcal{X}) \quad (28)$$

The notation $\Delta^g(\mathcal{X}, \mathcal{X})$ denotes the generalised inverse. $U_1 \succeq 0$ follows from standard properties of generalised Schur complements, as does the fact that $\Delta(\mathcal{X}', \mathcal{X}) \Delta^g(\mathcal{X}, \mathcal{X}) \Delta(\mathcal{X}, \mathcal{X}') = \Delta(\mathcal{X}', \mathcal{X}')$, which is required for Eq. (26) to hold. □

C Alternative constructions of NTKGP baselearners

To summarise the analysis in Section 3, the criteria for an NTKGP baselearner $\tilde{f}(\cdot, \theta)$ is that:

1) $\tilde{f}(\cdot, \theta_0) \xrightarrow{d} \mathcal{GP}(0, \Theta)$ as width increases, while 2) preserving the initial Jacobian $\nabla_\theta f_0(\cdot) = \nabla_\theta \tilde{f}_0(\cdot)$.

A possible alternative construction would be if one could (approximately) sample a fixed $f^* \sim \mathcal{GP}(0, \Theta)$, and set:

$$\tilde{f}_t(\cdot) = f_t(\cdot) + f^*(\cdot) - f_0(\cdot) \quad (29)$$

It is easy to approximately sample f^* for finite width NNs using a single JVP, under either standard or NTK parameterisation, by sampling $\tilde{\theta}$ independent of θ_0 and setting:

$$f^*(x) = \nabla_{\theta} f(x, \theta_0) \tilde{\theta} \quad (30)$$

Note that Eq. (29) requires computation of two forward passes f_t and f_0 in addition to a JVP $\nabla_{\theta} f(x, \theta_0) \tilde{\theta}$. For some implementations of JVPs, such as in JAX [30], the computation of f_0 will come essentially for free alongside the computation of $\nabla_{\theta} f(x, \theta_0) \tilde{\theta}$, because the JVP is centered about the same ‘‘primal’’ parameters θ_0 that are used for f_0 . Hence, this alternative \tilde{f} presented in Eq. (29) may have similar costs to our main construction in Section 3, for certain AD packages.

A second valid alternative to \tilde{f}_t would be to replace f_t with f_t^{lin} , which would give $\tilde{f}^{\text{lin}}(x, \theta_t) = \nabla_{\theta} f(x, \tilde{\theta}) \theta_t$ (where we swap $\tilde{\theta}$ and θ_0 for notational consistency with other NTKGP methods, and initialise at θ_0). Because $\tilde{\theta}$ is fixed, we see that $\tilde{f}^{\text{lin}}(\cdot, \theta_t)$ is linear in θ_t . This gives a realisation of the ‘‘sample-then-optimize’’ approach [29] to give posterior samples from randomly initialised linear models, and ensures that $\tilde{f}_{\infty}^{\text{lin}}(\cdot)$ is an exact posterior sample (using the empirical NTK $\hat{\Theta}_0$ as prior kernel) irrespective of parameterisation or width. Note though, of course, the linearised regime holds for \tilde{f}_t^{lin} throughout parameter space, hence for strongly convex optimisation problems like regression tasks with observation noise, the initialisation is irrelevant. We will call $\tilde{f}_{\infty}^{\text{lin}}$ trained in such a way an *NTKGP-Lin* baselearner.

D Regularisation in the NTKGP and RP training procedures

As stated in Lemma 3 of Osband et al. [22], suppose we are in a Bayesian linear regression setting with linear map $g_{\theta}(z) = z^{\top} \theta$, model $y = g_{\theta}(z) + \epsilon$ for $\epsilon \sim \mathcal{N}(0, \sigma^2)$ i.i.d., and parameter prior $\theta \sim \mathcal{N}(0, \lambda I_p)$. Then, having observed training data $\{(z_i, y_i)\}_{i=1}^n$, solving the following optimisation problem returns a posterior sample θ :

$$\tilde{\theta} + \operatorname{argmin}_{\theta} \sum_{i=1}^n \frac{1}{2\sigma^2} \left\| \tilde{y}_i - (g_{\theta} + g_{\tilde{\theta}})(z_i) \right\|_2^2 + \frac{1}{2\lambda} \|\theta\|_2^2 \quad (31)$$

where $\tilde{y}_i \sim \mathcal{N}(y_i, \sigma^2)$ and $\tilde{\theta} \sim \mathcal{N}(0, \lambda I_p)$.

We see that when there is a homoscedastic prior $\mathcal{N}(0, \lambda I_p)$ for θ that the correct weighting of L^2 regularisation is $\|\theta\|_{\Lambda}^2 = \frac{1}{\lambda} \theta^{\top} \theta$. In fact, even with a heteroscedastic prior $\theta \sim \mathcal{N}(0, \Lambda)$ with a diagonal matrix $\Lambda \in \mathbb{R}_+^{p \times p}$ and diagonal entries $\{\lambda_j\}_{j=1}^p$, it is straightforward to show that the correct setting of regularisation is $\|\theta\|_{\Lambda}^2 = \theta^{\top} \Lambda^{-1} \theta$ in order to obtain a posterior sample of θ . For RP-param or NTKGP-param methods, with initial parameters θ_0 , we have regularisation $\|\theta - \theta_0\|_{\Lambda}^2 = (\theta - \theta_0)^{\top} \Lambda^{-1} (\theta - \theta_0)$, which can be seen as a Mahalanobis distance.

For an NN in the linearised regime [21], this is related to the fact that the NTK and standard parameterisations initialise parameters differently, yet yield the same functional distribution for a randomly initialised NN. In the standard parameterisation, λ_j will be a factor of the NN width smaller than in the NTK parameterisation, but the corresponding feature map z will be a square root factor of the NN width larger. Thus, solving Eq. (31) will lead to the same functional outputs in both parameterisations, if the NN remains in the linearised regime. However, only with our NTKGP trained baselearners \tilde{f} do you get a posterior interpretation to the trained NN because of the difference between the NNGP and the NTK that standard training does not account for, and because the linearised regime only holds locally to the parameter initialisation.

E Other ensemble algorithms

Here, we present our ensemble algorithms for NTKGP-Lin (Algorithm 2) and NTKGP-fn (Algorithm 3), to complement the NTKGP-param algorithm that was presented in Section 3.4.

Algorithm 2 NTKGP-Lin ensemble

Require: Data $\mathcal{D} = \{\mathcal{X}, \mathcal{Y}\}$, loss function \mathcal{L} , NN model $f_{\theta} : \mathcal{X} \rightarrow \mathcal{Y}$, Ensemble size $K \in \mathbb{N}$, noise procedure: `data_noise`, NN parameter initialisation scheme: `init(·)`
for $k = 1, \dots, K$ **do**
 Form $\{\mathcal{X}_k, \mathcal{Y}_k\} = \text{data_noise}(\mathcal{D})$
 Initialise $\theta_k \stackrel{d}{\sim} \text{init}(\cdot)$
 Initialise $\tilde{\theta}_k \stackrel{d}{\sim} \text{init}(\cdot)$
 Define $\tilde{f}_k^{\text{lin}}(\mathbf{x}, \theta_t) = \nabla_{\theta} f(\mathbf{x}, \tilde{\theta}_k) \theta_t$ and set $\theta_0 = \theta_k$
 Optimise $\mathcal{L}(\tilde{f}_k^{\text{lin}}(\mathcal{X}_k, \theta_t), \mathcal{Y}_k) + \frac{1}{2} \|\theta_t - \theta_k\|_{\Lambda}^2$ for θ_t to obtain $\hat{\theta}_k$
end for
return ensemble $\{\tilde{f}_k^{\text{lin}}(\cdot, \hat{\theta}_k)\}_{k=1}^K$

Algorithm 3 NTKGP-fn ensemble

Require: Data $\mathcal{D} = \{\mathcal{X}, \mathcal{Y}\}$, loss function \mathcal{L} , NN model $f_{\theta} : \mathcal{X} \rightarrow \mathcal{Y}$, Ensemble size $K \in \mathbb{N}$, noise procedure: `data_noise`, NN parameter initialisation scheme: `init(·)`
for $k = 1, \dots, K$ **do**
 Form $\{\mathcal{X}_k, \mathcal{Y}_k\} = \text{data_noise}(\mathcal{D})$
 Initialise $\theta_k \stackrel{d}{\sim} \text{init}(\cdot)$
 Initialise $\tilde{\theta}_k \stackrel{d}{\sim} \text{init}(\cdot)$ and denote $\tilde{\theta}_k = \text{concat}(\{\tilde{\theta}_k^{\leq L}, \tilde{\theta}_k^{L+1}\})$
 Set $\theta_k^* = \text{concat}(\{\sqrt{2}\tilde{\theta}_k^{\leq L}, \tilde{\theta}_k^{L+1}\})$
 Define $\delta(\mathbf{x}) = \nabla_{\theta} f(\mathbf{x}, \theta_k^*) \theta_k^*$
 Define $\tilde{f}_k(\mathbf{x}, \theta_t) = f(\mathbf{x}, \theta_t) + \delta(\mathbf{x})$ and set $\theta_0 = \theta_k$
 Optimise $\mathcal{L}(\tilde{f}_k(\mathcal{X}_k, \theta_t), \mathcal{Y}_k) + \frac{1}{2} \|\theta_t\|_{\Lambda}^2$ for θ_t to obtain $\hat{\theta}_k$
end for
return ensemble $\{\tilde{f}_k(\cdot, \hat{\theta}_k)\}_{k=1}^K$

In Algorithm 3 we seek to reinitialise $\tilde{f}_k(\mathbf{x}, \theta_0)$ from $\mathcal{GP}(0, \mathcal{K})$ to $\mathcal{GP}(0, 2\Theta)$ in the infinite width limit, following the randomised prior function method of Osband et al. [22]. While there are many ways to do this we choose to use only one JVP, with a reweighted tangent vector, for $\delta(\cdot)$ in order to reduce extra computational costs. It would be similarly possible to model a scaling factor β for the prior function, like [22], using a single JVP with a differently reweighted tangent vector.

Note also that for the NTKGP-fn it is unreasonable to assume that the linearised NN dynamics will hold true for the duration of training because, unlike in NTKGP-param (Algorithm 1) we regularise towards the origin not the initialised parameters.

F Aggregating predictions from ensemble members

For completeness, we now describe how to aggregate predictions from ensemble members. Given a test point (\mathbf{x}, y) , for each baselearner NN $k \leq K$, we suppose we have a probabilistic prediction $p_k(y|\mathbf{x})$ obtained from the NN output. We then treat the ensemble as a uniformly-weighted mixture model over baselearners and combine predictions as $p(y|\mathbf{x}) = \frac{1}{K} \sum_{k=1}^K p_k(y|\mathbf{x})$. For our Bayesian deep ensembles, we can view this aggregation as a Monte Carlo approximation of the GP posterior predictive with NTK prior.

For classification tasks, this aggregation is exactly an average of predicted probabilities. For regression tasks, the prediction is a mixture of normal distributions, and we follow Lakshminarayanan et al. [11] by approximating the ensembled prediction as a single Gaussian with matched moments. That is to say, if $p_k(y|\mathbf{x}) \sim \mathcal{N}(\mu_k(\mathbf{x}), \sigma_k^2(\mathbf{x}))$, then we approximate $p(y|\mathbf{x})$ by $\mathcal{N}(\mu_*(\mathbf{x}), \sigma_*^2(\mathbf{x}))$ for $\mu_*(\mathbf{x}) = \frac{1}{K} \sum_k \mu_k(\mathbf{x})$ and $\sigma_*^2(\mathbf{x}) = \frac{1}{K} \sum_k (\mu_k^2(\mathbf{x}) - \mu_*^2(\mathbf{x})) + \sigma_k^2(\mathbf{x})$.

G Extra memory and computation costs of NTKGP methods

Of course, there is an extra cost to our NTKGP methods, which we will now compare to deep ensembles [11] and the randomised prior (RP) methods [22] for our implementations. In terms of computation, depending on the size of the dataset it might be feasible to run a single pass over the whole training set and store the additive corrections $\delta(\cdot)$ in a data loader. In this case, the training time computation of all methods would be similar. The left side of Table 2 compares the computational cost of different ensemble methods when this is not possible and the modified forward pass \tilde{f} needs to be computed on the fly, which is certainly the case at test time. A rule of thumb for an library offering forward-mode AD, like JAX [30], is that a JVP costs on the order of three standard forward passes in terms of FLOPs. It is worth pointing out that our methods share the same trainable parameters as standard deep ensembles, and so should not incur any additional computational cost in the backward pass.

Table 2: Comparison of computational and memory costs of different ensemble methods per ensemble member. Computational costs are specified per (modified) forward pass.

Method	Computational cost		Parameter sets to store	
	Forward passes	JVPs	Train time	Test time
Deep ensembles	1	0	1	1
RP-param	1	0	2	1
RP-fn	2	0	2	2
NTKGP-param	1	1	3	3
NTKGP-fn	1	1	3	3

In terms of memory, both the NTKGP and RP methods require storage of extra sets of parameters in order to compute the untrainable additive functions $\delta(\cdot)$ and regularise in parameter space, displayed in the right hand side of Table 2. However, the activations of the extra forward pass in the Randomised prior function method need not be stored. And moreover, forward mode JVPs are composed alongside the primitive operations that comprise the forward pass, so the memory requirements incurred by the extra JVP are independent of the NN depth for our NTKGP methods.

It is undeniable that our methods suffer from increased memory and computational costs relative to deep ensembles, which is already known to be an expensive method in practice [48], and the RP methods to a lesser extent. However, it is worth pointing out that our Bayesian deep ensembles still retain the distributability of standard deep ensembles. Moreover, our computational and memory costs still scale linearly in dataset size and parameter space dimension, enabling us to work with large scale datasets like Flight Delays [38].

H Experimental Details & additional plots

H.1 Toy 1d example

We set ensemble size $K = 20$, and train on full batch GD with learning rate 0.001 for 50,000 iterations under standard parameterisation in Neural Tangents [33], with $\sigma_W = 1.5$ & $\sigma_b = 0.05$, for σ_W, σ_b defined as in Appendix A.

H.2 Flight Delays

Our baselearners are MLPs with 4 hidden layers, 100 hidden units per layer and ReLU activations, and we use standard parameterisation with $\sigma_W = 1$ & $\sigma_b = 0.05$, and choose ensemble size $K = 5$. We train for 10 epochs with learning rate 0.001, batch size 100 and Adam [49]. All methods apart from deep ensembles are L^2 regularised according to Appendix D, with weight decay strength set to 10^{-4} for deep ensembles.

We use a validation set of size 50k that is sampled uniformly from the training set of size 700k, and early stop baselearner NNs based on validation set loss. It would also be possible to use a validation

set to tune hyperparameters of the NTK, though we leave this for future work; see Fong and Holmes [50] for a connection between cross-validation and marginal likelihood maximisation. Inputs and targets are standardised so that the training data is zero mean and unit variance.

H.3 MNIST vs. NotMNIST

Baselearners are MLPs with 2-hidden layers, 200 hidden units per layer and ReLU activations. We use standard parameterisation with $\sigma_W = 1.5$ & $\sigma_b = 0.05$, and set label smoothing to 0.1, so one-hot labels are transformed as $y \leftarrow 0.1 \frac{1_C}{C} + 0.9y$. No L^2 regularisation is added, which means the RP-param method is no different to deep ensembles, hence we omit RP-param from our MNIST experiments. We train for 20 epochs with batch size 100, learning rate 0.01 and Adam [49].

Figure 4 compares different ensemble methods for in terms of the entropy of predictive probabilities on both MNIST and NotMNIST test sets. We see that, as expected, our NTKGP methods make more conservative predictions for both MNIST and NotMNIST.

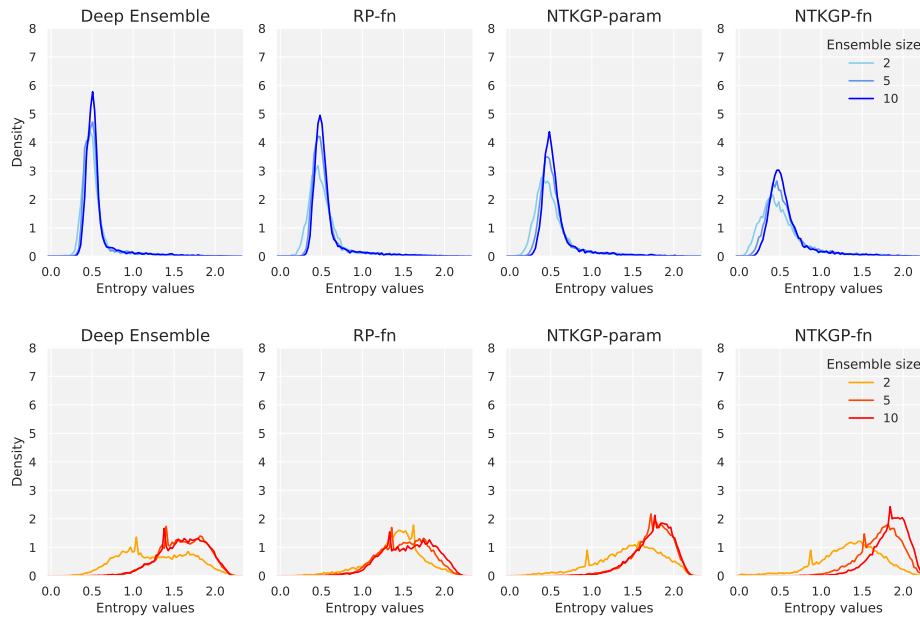


Figure 4: Histograms of predictive entropy on MNIST (top) and NotMNIST (bottom) test sets for different ensemble methods and for different ensemble sizes.